Larhyss Journal, ISSN 1112-3680, n°54, Jun 2023, pp. 145-174

CONTROL OF THE HYDRAULIC JUMP BY A BROAD-CRESTED SILL IN A RECTANGULAR CHANNEL NEW THEORY AND EXPERIMENT

ACHOUR B.[1*], AMARA L.[2]

[1] Research Laboratory in Subterranean and Surface Hydraulics (*LARHYSS*), University of Biskra, Algeria,
[2] Department of Civil Engineering and Hydraulics, Faculty of Science and Technology, University of Jijel, Algeria,

(*) bachir.achour@larhyss.net

Research Article – Available at http://larhyss.net/ojs/index.php/larhyss/index
Received February 10, 2023, Received in revised form June 2, 2023, Accepted June 4, 2023

ABSTRACT

The present research focuses on hydraulic jumps of initial and final depths h_1 and h_2, respectively, controlled by a broad-crested sill of height s in a horizontal rectangular channel. The main objective is to know which parameters influence the height of the sill in such a way as to create a full hydraulic jump on the stilling basin. First, the study reviews the essential works of Forster and Skrinde published in 1950, which are still in force today. An in-depth study of these works shows that the theoretical development carried out by the aforementioned authors is based on two simplifying assumptions that risk compromising the reliability of the derived equations, in particular, that govern the relative sill height $S = s/h_1$, as a function of the incident Froude number F_1. A detailed and appropriate calculation shows that this relationship is not recommendable and therefore requires an adjustment.

For this, a much more rigorous theoretical development is proposed, which leads to establishing a surrogate relationship safely allowing the explicit calculation of the relative sill height value required for the formation of the hydraulic jump on the stilling basin. Contrary to what has been proposed by previous studies, the current theoretical development takes into account the effect of the approach flow velocity immediately upstream of the sill.

This effect is represented by the dimensionless parameter σ defined as a kinetic factor. The calculation showed that for a wide range of incident Froude numbers, the kinetic factor cannot be neglected. A table comparing the values of the relative sill height S calculated according to Forster and Skrinde and the current approach shows that the

maximum deviation observed for $\sigma \neq 0$ is significant, reaching 26.15% for $F_1 = 3$ and 8.41% for $F_1 = 11$. If the effect of the approach flow velocity was to be neglected, which corresponds to $\sigma = 0$, the maximum deviation could reach 5%, which is not insignificant.

The second part of the study is devoted to the experimental investigation. It has the main objective of corroborating or correcting the theoretical relationships developed during the first part. For this, a specially designed easy and efficient hydraulic installation is put into operation, highlighting an original device generating an incident flow of high velocity. It consists of a pressurized box-convergent assembly directly fed by a pump via a flexible pipe.

The analysis of the experimental measurements shows that the theoretical sequent depth ratio Y of the hydraulic jump, according to Belanger's equation, is not affected by the setup of the broad-crested sill. Everything happens as if the sill does not exist. Thus, it seems that the sill is only useful in controlling the position of the hydraulic jump such that it forms completely on the horizontal apron.

Moreover, the accuracy of the new rigorous derived theoretical relationship $S(F_1)$ is experimentally confirmed.

Keywords: Forster and Skrinde, Broad-crested sill, Control of hydraulic jump, Horizontal apron, Kinetic factor.

INTRODUCTION

Many hydraulic structures, such as shaft spillways or surface spillways, evacuate water and return it further downstream in the water stream. This evacuation results, in most cases, in the transformation of the potential energy stored by the reservoir into strong kinetic energy upstream of the release structure. The generated erosive forces, which are proportional to the square of the velocity, can seriously threaten the structure by their strongly erosive nature, and it is then often required to dissipate this kinetic energy in the greatest possible proportion. At the entrance to the release structure, the flow is in a supercritical regime characterized by an incident Froude number greater than unity. The principle of dissipation consists of transforming this supercritical regime into a subcritical regime characterized by low velocities downstream of the structure known as an "energy dissipator" or "stilling basin", i.e., a device designed to protect downstream areas from erosion by reducing the velocity of flow to acceptable limits. A hydraulic jump then arises over the entire length of the stilling basin, often rectangular in shape and sometimes equipped with obstacles such as baffles and continuous or toothed sills, deliberately placed according to the width of the basin.

The purpose of the sill is to prematurely cause the formation of the hydraulic jump and to control its position during flow rate changes so that it does not move either upstream or downstream of the stilling basin. Hydraulic jumps controlled by sills were first studied in rectangular channels before being extended to other channel profiles, such as triangular

channels and U-shaped channels (Forster and Skrinde, 1950; Hager and Li, 1992; Achour et al., 2002; Achour and debabèche, 2003a; Achour and Debabèche, 2003b). On this subject, Peterka (1983) compiled an excellent monograph describing the various types of stilling basins encountered in hydraulic engineering practice.

Almost a decade later, Nandana and Ayed (1992) improved the performance of the type III stilling basin, following the USBR classification, and provided a new design method. The tested basin, called modified type III, has an additional row of toothed sills, and the distribution of velocities in the subcritical flow downstream of the hydraulic jump is thus improved.

The hydraulic jump originating in a basin equipped with one or more sills, continuous or discontinuous, is said to be controlled (Forster and Skrinde, 1950) and sometimes even forced (Bretz, 1988), as opposed to the classic jump formed on a horizontal apron of rectangular cross-section and devoid of any obstacle (Hager et al., 1990). This type of jump is often referred to in the literature as "A jump" (Bretz, 1988).

The main characteristics of a classical or controlled hydraulic jump are the yield or the efficiency represented by the ratio of the total head loss they cause to the total head in their initial section, their characteristic lengths and their initial and final depths. From a quantitative point of view, the characteristics of the hydraulic jump essentially depend on the geometry of the stilling basin, the incident Froude number and the relative sill height $S = s/h_1$ in the case where the hydraulic jump is controlled or forced; s and h_1 represent the sill height and the initial depth of the hydraulic jump, respectively (Bretz, 1988; Achour 1997).

For economic and efficiency reasons, the hydraulic jump must extend over a shorter length; that is, the basin must be compact, provide the smallest possible final downstream height and finally dissipate the maximum amount of energy (Hager and Li, 1992; Bretz, 1988).

The study carried out by Hager and Wanoschek (1987) shows that, for a given value of the incident Froude number, the hydraulic jump in a triangular channel is characterized by greater efficiency and by a lower sequent depth ratio $Y = h_2/h_1$ than that of the hydraulic jump evolving in rectangular and trapezoidal channels, where h_2 is the final depth of the hydraulic jump. The literature shows, however, that the interest of research workers has focused essentially on the hydraulic jump evolving in a rectangular channel, no doubt because of the geometric simplicity of such a structure and its ease of implementation both from practical and experimental points of view.

All studies on the hydraulic jump have confirmed that it is governed by the momentum equation, although the velocity distribution is not uniform downstream of the hydraulic jump, i.e., immediately upstream of the sill. Apart from a few studies, such as that of Smith and Chen (1989) for the hydraulic jump in a steeply sloping square conduit, the study of McCorquodale and Mohamed (1994) on the hydraulic jump on an adverse slope, that of Kawagoshi and Hager (1989) on the B-jump in a sloping channel, or that of Achour (Achour, 1997; Achour, 2000) related to the hydraulic jump in a suddenly widened

circular tunnel, the application of the momentum equation essentially concerned the type A jump originating on a horizontal apron or which could be considered as such because of its low bed slope (Bretz, 1988). The tangential component of the proper weight of the liquid mass constituting the hydraulic jump, which is difficult to evaluate from a theoretical point of view in the general case, no longer needs to be taken into consideration. Moreover, the effect of friction is neglected compared to the head loss caused by the hydraulic jump. With all these simplifications, the application of the momentum equation generally causes no major problems.

The considerations set out above led to the establishment of the universally known Belanger's relationship (1828), allowing the explicit calculation of the sequent depth ratio Y as a function of the incident Froude number F_1 for the case of the classical hydraulic jump.

Regarding the hydraulic jump controlled by a broad-crested sill in a rectangular channel, Forster and Skrinde (1950) were the first to propose a purely theoretical approach. To date, no study has brought new arguments to corroborate or invalidate this approach. As stated by Forster and Skrinde (1950), the hydraulic jump controlled by a broad-crested sill is no exception since it is also governed by the momentum equation applied between the final section of the jump and a selected section of the flow above the sill where the depth is minimal. However, two simplifying assumptions were the basis of the theoretical development. The first admits that the effect of the approach flow velocity is negligible, while the second imposes a restriction on the minimum depth of the flow above the sill. Since then, there have been no other studies, either from theoretical or experimental points of view, which could have corroborated or possibly corrected the theoretical relationships proposed by these authors by observing the side effect of the abovementioned hypotheses on the momentum equation.

Our in-depth research in the specialist literature clearly confirms that the work of Forster and Skrinde (1950) is the only means used today for the design of stilling basins working with hydraulic jumps controlled by a sill, both broad and thin-crested. Applying the momentum equation to the case of a broad-crested sill controlling the hydraulic jump in a rectangular channel, which is of interest to the present study, Forster and Skrinde (1950) derived the implicit theoretical relationship between the relative sill height S and the incident Froude number F_1 based on the simplifying assumptions previously pointed out. Thus far, design engineers have used this relationship to derive the required value of the sill height s provided that the incident Froude number F_1 is given.

The current research will reveal, from the theoretical and experimental points of view, that the Forster and Skrinde development is not rigorous or even not advisable. Thus, a much more convincing surrogate relationship derived from rigorous theoretical development devoid of any simplifying assumptions is proposed, highlighting the harmful influence of the simplifying assumptions of the Forster and Skrinde approach and the shortcomings of the resulting equation.

AVAILABLE RELATIONSHIPS

The sill is considered "broad" when the liquid profile flowing through is almost parallel to the crest of the sill, provided that the length L is sufficient (Fig. 1).

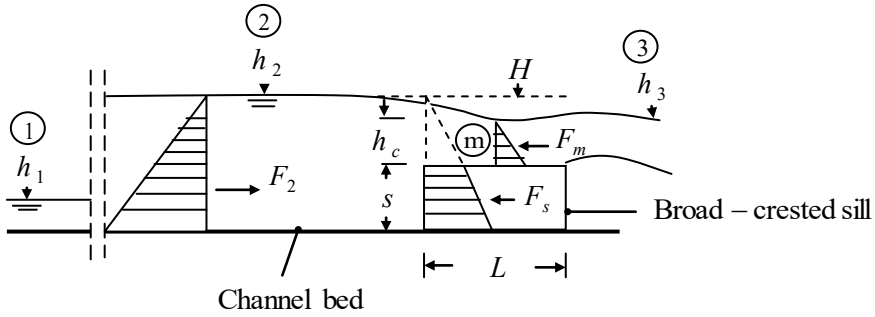

Figure 1: Crossing flow with a continuous broad-crested sill of height s and length L. The hatched surfaces correspond to the assumed hydrostatic distribution of pressures

The concept of the broad-crested sill is also related to the characteristics of the flow, and according to the classification of Rao and Muralidhar (1963), the sill is considered to be broad if the following condition is satisfied:

$$0.10 \le \frac{h_2 - s}{L} \le 0.35 \tag{1}$$

In section 2 of Fig. 1, the flow is in the subcritical regime of depth h_2. The depth $h_2$could be the final depth of a classical hydraulic jump with initial depth h_1 in section 1 (Fig. 1), generated by a sluice gate, for instance, or by any other incident flow generating device. The sill is then crossed by a flow in the critical regime of depth h_c, followed by a slice of flow in the supercritical regime whose final depth h_m is the smallest possible in section m, i.e., minimum. The external forces that act on the chosen sections 2 and m are the following: the hydrostatic force F_2 applied to section 2 upstream of the sill; the reaction force F_s applied on the upstream face of the sill, and the hydrostatic force F_m applied to section m. Per unit channel width, these forces are expressed, respectively, as:

$$F_2 = \frac{1}{2}\rho g\, h_2^2 \tag{2}$$

$$F_s = \frac{1}{2}\rho g\, s\left[h_2 + \left(h_2 - s\right)\right] \tag{3}$$

$$F_m = \frac{1}{2}\rho g\, h_m^2 \tag{4}$$

where ρ is the density of the flowing liquid (kg.m^{-3}) and g is the acceleration due to gravity (m.s^{-2}).

If one considers that all the friction forces are negligible, that the depth h_m is the minimum depth on the threshold and that the pressure distribution is hydrostatic, then the application of the momentum equation allows writing the following:

$$\frac{q}{g}\left(\frac{q}{h_m}-\frac{q}{h_2}\right)=\frac{h_2^2}{2}-\frac{h_m^2}{2}-\frac{s\left[h_2+\left(h_2-s\right)\right]}{2} \tag{5}$$

where q is the discharge per unit width (m^2.s^{-1}), that is, the discharge Q (m^3.s^{-1}) divided by the width b of the channel (m).

On the other hand, tests performed by Doeringsfeld and Barker (1941) showed the following:

$$(h_2 - s) \cong 2h_m \tag{6}$$

Under this condition, the momentum equation expressed by (5) reduces to:

$$q = 0.433\sqrt{2g}\,\frac{h_2}{h_2+s}H^{3/2} \tag{7}$$

where:

$$H = h_2 - s \tag{8}$$

As shown in Fig. 1 as well as Eq. (8), H represents the vertical distance counted above the sill without taking into account the velocity head $\frac{V_2^2}{2g}$, which amounts to saying that the approach flow velocity has been neglected.

The classical hydraulic jump is governed by the well-known Belanger equation (1828), which expresses the sequent depth ratio Y in terms of the incident Froude number F_1 as follows:

$$Y=\frac{1}{2}\left(\sqrt{1+8F_1^2}-1\right) \tag{9}$$

Combining Eqs. (7), (8), and (9), and knowing that $F_1^2 = \frac{q^2}{gh_1^3}$ results in:

$$\frac{21.33\,F_1^2}{\sqrt{1+8F_1^2}-1}=\frac{\left(\sqrt{1+8F_1^2}-1-2\,s/h_1\right)^3}{\sqrt{1+8F_1^2}-1+2\,s/h_1} \tag{10}$$

Thus, Eq. (10) attributed to Forster and Skrinde (1950) shows that the relative sill height S is an implicit function of the incident Froude number F_1. Using an iterative process

applied to Eq. (10), Table 1 has been drawn up which allowed plotting Fig. 2 representing the variation in S as a function of F_1.

Table 1: Values of the relative sill height S as a function of F_1 according to Forster and Skrinde implicit Eq. (10)

F_1	$S = \frac{s}{h_1}$
3	0.715
4	1.395
5	2.136
6	2.921
7	3.739
8	4.585
9	5.454
10	6.342
11	7.246

Figure 2: Variation in the relative sill height S as a function of F_1 according to Table.1

As shown in both Table 1 and Fig. 2, the relative sill height S increases with the increase in the incident Froude number $\boldsymbol{F_1}$. When the Froude number $\boldsymbol{F_1}$ increases, the hydraulic jump moves downstream and then disappears, giving way to a supercritical flow over the stilling basin. To make the hydraulic jump reappear, it is necessary to increase the height s of the sill.

The curve of Fig. 2 can be used provided that the depth h_3 downstream of the sill, in section 3, satisfies the following inequality:

$$h_3 < \frac{1}{3}\left(2h_2 + s\right) \tag{11}$$

Forster and Skrinde (1950) also note that the curve in Fig. 2 coincides with that obtained for the case of the hydraulic jump controlled by a positive step crossed by a critical flow of depth h_c and such that the length of the stilling basin is as follows:

$$X = 5\left(s + h_c\right) \tag{12}$$

NEW THEORETICAL APPROACH

Let us assume that Fig. 1 represents a classical hydraulic jump generated by a sluice gate and controlled by a broad-crested sill crossed in a critical regime. The indicated sections 1 and 2 are the initial and final sections of the hydraulic jump, respectively. Taking the horizontal bottom of the channel as the reference plane and considering the kinetic energy correction coefficient equal to unity, the total heads H_1 and H_2 in sections 1 and 2 are written, respectively, as:

$$H_1 = h_1 + \frac{V_1^2}{2g} \tag{13}$$

$$H_2 = h_2 + \frac{V_2^2}{2g} \tag{14}$$

From the geometric point of view, Fig. 1 shows the following:

$$H_2 = s + H_c = s + 1.5h_c \tag{15}$$

The head loss ΔH due to the hydraulic jump is given by the difference between the heads H_1 and H_2 such that:

$$\Delta H = H_1 - H_2 \tag{16}$$

Combining Eqs. (15) and (16) yields what follows:

$$\Delta H = H_1 - \left(s + 1.5h_c\right) \tag{17}$$

Let us consider the following dimensionless parameters:

$$\Delta H^* = \frac{\Delta H}{h_c} \tag{18}$$

$$H_1^* = \frac{H_1}{h_c} \tag{19}$$

$$h_1^* = \frac{h_1}{h_c} \tag{20}$$

$$h_2^* = \frac{h_2}{h_c} \tag{21}$$

Thus, Eq. (17) reduces to:

$$\frac{s}{h_1} = \frac{H_1^* - \Delta H^* - 3/2}{h_1^*} \tag{22}$$

However, the Froude number F_1 of the incident flow can be written as follows:

$$F_1 = \frac{1}{h_1^{*\,3/2}} \tag{23}$$

In the same way, considering Eq. (13), one may derive the following:

$$H_1^* = \frac{H_1}{h_c} = h_1^* + \frac{1}{2h_1^{*\,2}} \tag{24}$$

Belanger's equation (9) can be transformed into the following form:

$$h_2^* = \sqrt{h_1^{*\,2}/4 + 2/h_1^*} - h_1^*/2 \tag{25}$$

It is well known that the head loss ΔH due to the classical hydraulic jump is expressed as (Bretz, 1988):

$$\Delta H = \frac{\left(h_2 - h_1\right)^3}{4h_2 h_1} \tag{26}$$

Eq. (26) can be rewritten as follows:

$$\Delta H^* = \frac{\left(h_2^* - h_1^*\right)^3}{4h_2^* h_1^*} \tag{27}$$

Considering Eqs. (23), (24), (15), and (27), Eq. (22) then clearly shows that the relative sill height S only depends on the incident Froude number F_1.

Identically to Eq. (24), one may write that:

$$H_2^* = \frac{H_2}{h_c} = h_2^* + \frac{1}{2h_2^{*2}} \tag{28}$$

Eq. (28) can be rewritten as follows:

$$H_2^* = Y h_1^* + \frac{1}{2Y^2 h_1^{*2}} \tag{29}$$

Eq. (18) can be easily written as follows:

$$\Delta H^* = H_1^* - H_2^* \tag{30}$$

Thus, Eq. (22) becomes:

$$\frac{s}{h_1} = \frac{H_2^* - 3/2}{h_1^*} \tag{31}$$

Combining Eqs. (23), (29), and (31) results in:

$$\frac{s}{h_1} = \left(\frac{Y}{F_1^{2/3}} + \frac{F_1^{4/3}}{2Y^2} - 3/2 \right) F_1^{2/3} \tag{32}$$

After simplifications, Eq. (32) reduces to:

$$\frac{s}{h_1} = Y + \frac{1}{2}\left(\frac{F_1}{Y} \right)^2 - \frac{3}{2} F_1^{2/3} \tag{33}$$

What is known in practice is the incident Froude number F_1, and the relationship (33) allows the direct calculation of the height s of the sill required for the complete formation of the hydraulic jump on the stilling basin.

In a previous study performed on the control of hydraulic jumps in a U-shaped channel (Achour and debabèche, 2003b), the rectangular channel was considered a special case, and the relationship (33) was deduced.

Let us remember that the sequent depth ratio Y is related to the incident Froude number F_1 by Belanger's Eq. (9).

For the value F_1=1, corresponding to the critical flow condition, Belanger's Eq. (9) gives Y = 1. Consequently, Eq. (33) allows us to write that S = 0. It is not possible to satisfy these conditions from Forster and Skrinde's Eq. (10) because this is an incomplete approximate relationship.

Eq. (33) confirms what was stated earlier, namely, the relative sill height S depends solely on the Froude number F_1. This is the same conclusion reached by Forster and Skrinde through their relationship (10); however, Eqs. (10) and (33) are fundamentally different.

The first equation is based on two simplifying assumptions, namely, the approach flow velocity is neglected, and the minimum height h_m is approximately given by Eq. (6). These simplifying assumptions could significantly reduce the reliability of Eq. (10). Contrariwise, Eq. (33) is not based on any simplifying assumption; in particular, it takes into account the approach flow velocity. On the other hand, Eq. (10) is implicit in *S*, which further complicates the calculation of this parameter. For the computation of *S*, it is necessary to use a calculation program based on iterative procedures. Thus, the other significant advantage of Eq. (33) is that it is explicit, allowing the direct computation of *S* for a given value of the incident Froude number F_1.

The values of the relative sill height *S*, computed according to Eqs. (10) and (33), are grouped together in comparative Table 2 for the wide range of incident Froude numbers, such as $3 \leq F_1 \leq 11$. The deviations caused by these two relationships are also reported.

Table 2: Values of the relative sill height *S* according to Forster and Skrinde's Eq. (10) and the author's Eq. (33)

F_1	$S = \frac{s}{h_1}$ Eq. (10)	$S = \frac{s}{h_1}$ Eq. (33)	Deviation (%)
3	0.715	0.968	26.15
4	1.395	1.697	17.81
5	2.136	2.490	14.24
6	2.921	3.328	12.24
7	3.739	4.200	10.97
8	4.585	5.098	10.06
9	5.454	6.018	9.37
10	6.342	6.957	8.84
11	7.246	7.912	8.41

Table 2 shows that Eq. (33) derived from the theoretical authors' approach gives relative sill height values greater than those resulting from Forster and Skrinde's approximate Eq. (10). However, the observed deviation decreases as the incident Froude number F_1 increases. These deviations could be partly explained by the fact that the approach flow velocity was neglected in the theoretical development carried out by Forster and Skrinde. It is useful to note indeed that the following quantity that appears in Eq. (33):

$$\sigma = \frac{1}{2}\left(\frac{F_1}{Y}\right)^2 \tag{34}$$

is closely related to the kinetic energy downstream of the hydraulic jump since one may write that:

$$\sigma = \frac{1}{2}\left(\frac{F_1}{Y}\right)^2 = \frac{V_2^2}{2\,g\,h_1} \tag{35}$$

where V_2 is the mean flow velocity in section 2 shown in Fig. 1.

Table 3 groups the values of the kinetic factor σ calculated according to Eq. (35) for the wide range $3 \leq F_1 \leq 11$.

Table 3: Values of the kinetic factor σ as a function of the incident Froude number according to Eq. (35)

F_1	σ Eq. (35)
3	0.3163
4	0.2983
5	0.2880
6	0.2812
7	0.2765
8	0.2731
9	0.2704
10	0.2683
11	0.2666

As shown in Table 3, the kinetic factor σ decreases as the incident Froude number F_1 increases while varying in the range $0.267 \leq \sigma \leq 0.316$. The values of σ indicated in this range are not insignificant, which allows us to conclude that the approach flow velocity cannot be neglected. If σ were deliberately neglected, i.e., $\sigma = 0$, Eq. (33) would be reduced to:

$$\frac{s}{h_1} = Y - \frac{3}{2}F_1^{2/3} \tag{36}$$

This would lead to a maximum deviation of approximately 5% in comparison to the values of the relative sill height S computed using Forster and Skrinde's Eq. (10) and reported in Table 2.

Fig. 3 shows both the variation curves of the relative height S of the broad-crested sill as a function of the incident Froude number F_1, according to Forster and Skrinde Eq. (10) and the authors' Eq. (33) for $\sigma = 0$ and $\sigma \neq 0$.

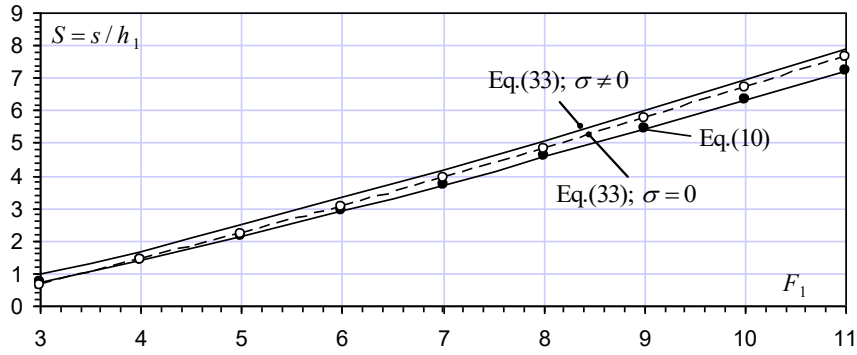

Figure 3 : Variation $S(F_1)$. (–) Author's Eq. (33) for $\sigma \neq 0$; (- - o - -) Author's Eq.(33) for $\sigma = 0$; (–•–) Forster and Skrinde's approximate Eq.(10)

Let us assume that ΔS represents the deviation between the value of the relative sill height S corresponding to $\sigma \neq 0$ and $\sigma = 0$, i.e.,

$$\Delta S = S_{\sigma \neq 0} - S_{\sigma = 0} \tag{37}$$

Taking into account Eq. (33), Eq. (37) becomes:

$$\Delta S = Y + \frac{1}{2}\left(\frac{F_1}{Y}\right)^2 - \frac{3}{2}F_1^{2/3} - Y + \frac{3}{2}F_1^{2/3} \tag{38}$$

After simplifications, Eq. (38) reduces to:

$$\Delta S = \frac{1}{2}\left(\frac{F_1}{Y}\right)^2 = \sigma \tag{39}$$

Eq. (39) indicates that ΔS corresponds to the kinetic factor σ. Inserting Eq. (9) into Eq. (39) results in:

$$\Delta S = \sigma = \frac{2F_1^2}{\left[\sqrt{1+8F_1^2} - 1\right]^2} \tag{40}$$

Eq. (40) clearly shows that ΔS depends solely on the incident Froude number F_1. The variation of $\Delta S = \sigma$ as a function of F_1 is shown graphically in Fig. 4 in accordance with Eq. (40). This shows that ΔS undergoes a rapid decrease in the range $1 < F_1 \leq 5$ and then a slow decrease beyond $F_1 = 5$.

The relative deviation on the relative sill height S is written as:

$$\frac{\Delta S}{S_{\sigma=0}} = \frac{\sigma}{S_{\sigma=0}} = \frac{S_{\sigma\neq 0} - S_{\sigma=0}}{S_{\sigma=0}} \tag{41}$$

Eq. (41) is also represented in Fig. 4, showing that $\frac{\Delta S}{S_{\sigma=0}}$ decreases as F_1 increases and takes the value of 4.7% (0.047) for $F_1 = 9$.

The point of intersection of the two curves in Fig. 4 translates the following equality:

$$\frac{\Delta S}{S_{\sigma=0}} = \Delta S \tag{42}$$

This amounts to writing that:

$$S_{\sigma=0} = 1 \tag{43}$$

Inserting the previous condition into Eq. (33) yields:

$$Y - \frac{3}{2} F_1^{2/3} - 1 = 0 \tag{44}$$

Taking into account Eq. (9) expressing $Y(F_1)$, the calculation shows that the root of Eq. (44) is:

$$F_1 = 3.4771 \tag{45}$$

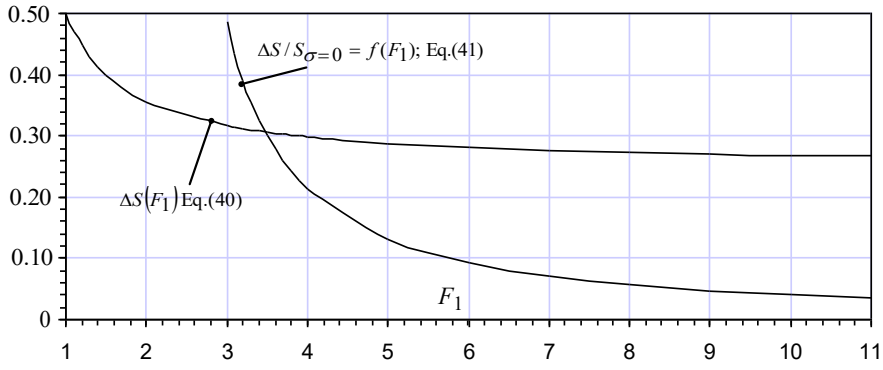

Figure 4: Variation in ΔS = σ and $\Delta S/S_{(\sigma=0)}$ as a function of the incident Froude number F_1.

It is worth noting that although Eq. (10) is not recommended for the objective reasons previously pointed out; however, its implicit character can be lifted by replacing it with the implicit modified model of Hoerl (Kolb, 1983) such that:

$$S = 0.5861 \times 0.1384^{1/F_1} F_1^{1.1433} - 0.3494 \tag{46}$$

The calculation showed that in the wide range $3 \le F_1 \le 11$, the maximum deviation caused by the use of the explicit Eq. (46) is less than 0.038% when compared to the implicit Eq. (10).

EXPERIMENTAL VALIDATION

Description of the flow and problem statement

The objective of this part of the study consists of the experimental investigation of the hydraulic jump controlled by the setup of a continuous broad-crested sill. The theoretical relationships derived previously will be subjected to an experimental program as intensely as it is rigorous to corroborate them or correct them if deviations are observed between the theoretical and experimental results. Instead of generating an incident flow through a sluice gate, as in most previous studies, a specially designed device consisting of a box-convergent assembly working under a pressurized state was used (Figs. 5, and 6). The box as well as the convergent are equipped with steering guides that properly direct the flow toward the entrance of the channel. The box is fed directly by the pump using piping. The entire device is constructed by welding metal plates of sufficient thickness to ensure the nondeformability of the system. Such a device has many advantages; in particular, it generates a high-velocity incident flow, and the initial flow outlet height h_1, i.e., the initial depth of the hydraulic jump, is controlled by the exit opening a_o of the convergent element (Fig. 5)

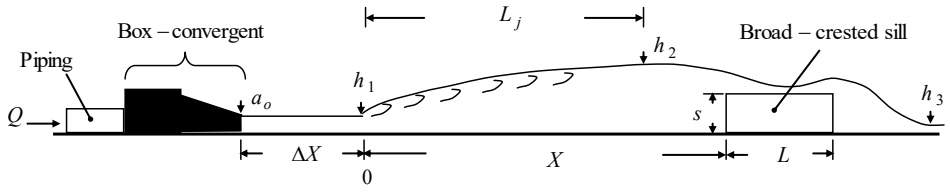

Figure 5: Hydraulic jump controlled by a broad-crested sill; incident flow generated by a box-convergent set

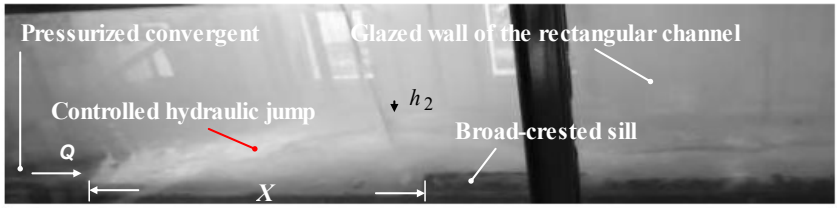

Figure 6: Photograph illustrating an experimental configuration of a controlled hydraulic jump by a broad-crested sill

The implementation of a broad-crested sill of height s and length L in a rectangular channel of width b, placed at a distance X from the initial section of the hydraulic jump, makes this one appear on the horizontal apron of the channel.

For a given value of the incident Froude number F_1 and for a chosen sill height s, the hydraulic jump starts at the origin 0 and extends over the length L_j less than the horizontal distance X (Fig. 1). The increase in the Froude number F_1, due to the increase in the flow rate Q, causes both the displacement of the jump downstream as well as the increase in its length L_j. If the length ΔX is short enough, the initial depth h_1 of the hydraulic jump can be assimilated to the outlet opening a_o of the convergent. Incident flow can also be generated by a sluice gate, and the initial depth of the jump is such that $h_1 = C_c a_o$, where $C_c$denotes the coefficient of contraction of the sluice gate and a_o the opening thereof. On the other hand, if the length ΔX is large, the initial depth h_1 must be measured at origin 0. The flow slice spanning the distance ΔX is both supercritical and gradually varies. It is in fact an H_3-type backwater curve because the channel apron is horizontal.

Despite the increase in the incident Froude number, the flow slice of length ΔX can be reduced by raising the sill, i.e., by increasing the sill height s. The increase in both the incident Froude number F_1 and the sill height s implies an increasingly large relative length L_j / X which would be equal to unity as a limit value. The greater the length X is, the higher the values of the incident Froude number F_1 and of the sill height s must be to obtain a relative length L_j / X equal to unity.

To reach the state of the flow described in Fig. 1, it is necessary to go through a number of experimental manipulations.

The test channel is fed at an increasing flow rate Q. The horizontal apron is first flooded as shown in Fig. 7.

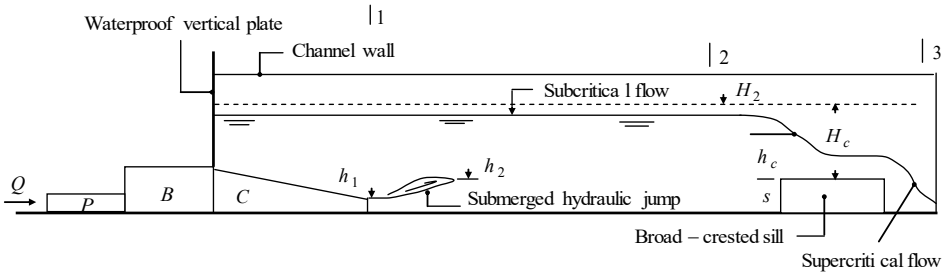

Figure 7: Mechanism of formation and appearance of the hydraulic jump in a flooded basin with increasing flow rate *Q*. *P*: Piping; *B*: pressurized box; *C*: pressurized convergent.

The flow is in a subcritical regime on the horizontal apron, critical above the sill, and supercritical downstream thereof. The mean velocity V_1 of the flow exiting convergent *C* is lower than the critical velocity V_c, i.e.,

$$V_1 < V_c \tag{47}$$

The velocities V_1 and V_c are written as follows:

$$V_1 = \frac{Q}{b\,h_1} \tag{48}$$

$$V_c = \frac{Q}{b\,h_c} \tag{49}$$

where h_1 denotes the thickness of the water vein coming out of convergent *C*, which also corresponds to the initial depth of the hydraulic jump as defined previously, and h_c is the critical depth. Thus, inequality (47) allows us to write the following:

$$h_c < h_1 \tag{50}$$

This reflects the subcritical nature of the flow in section 1 (Fig. 7). In this section, the incident Froude number F_1 is less than unity, i.e.,

$$F_1 = \left(\frac{Q^2}{g\,b^2\,h_1^3} \right)^{1/2} < 1 \tag{51}$$

That is,

$$Q < b\sqrt{g}\,h_1^{3/2} \tag{52}$$

The total head of the liquid stream in the subcritical regime between convergent *C* and the sill of height *s* is written as:

$$H_{Sub} = s + H_c \tag{53}$$

where the subscript "*Sub*" denotes "Subcritical", and H_c is the critical total head above the sill. On the other hand, neglecting all head losses that might occur both inside convergent *C* and in the abrupt vertical enlargement at the exit of the convergent, the total head upstream of convergent *C* is approximately such that:

$$H_{Up} = H_{Sub} + \frac{V_1^2}{2g} \tag{54}$$

where the subscript "*Up*" denotes "Upstream".

Eq. (54) can be rewritten as:

$$H_{Up} = H_{Sub} + \frac{Q^2}{2g\,b^2\,h_1^2} \tag{55}$$

The critical depth h_c in a rectangular channel is written as:

$$h_c = \left(\frac{Q^2}{g\,b^2}\right)^{1/3} \tag{56}$$

Consequently, Eq. (55) becomes:

$$H_{Up} = H_{Sub} + \frac{h_c^3}{2\,h_1^2} \tag{57}$$

Combining Eqs. (50) and (57) results in:

$$H_{Up} < H_{Sub} + \frac{h_c^3}{2} \tag{58}$$

Inserting Eq. (53) into Eq. (58) yields:

$$H_{Up} < s + H_c + \frac{h_c^3}{2} \tag{59}$$

By increasing the flow rate *Q*, the flow velocity in section 1 at the exit of convergent *C* increases. When the flow velocity V_1 in this section exceeds the critical velocity V_c, i.e., when $V_1 > V_c$ and $h_c > h_1$, the flow regime of the liquid vein leaving convergent *C* becomes supercritical to transform into a subcritical flow between sections 1 and 2. This implies the existence of a localized hydraulic jump between these sections, but it will remain

submerged as long as the depth $h_2$of the roller is below the water level imposed by the total head$H_2 = s + H_c$, or as long as:

$$h_2 < h_{2;Sub} \tag{60}$$

One may also state that the water whirlpool, like a premature hydraulic jump, occurring at the exit of convergent *C* will remain submerged as long as the water head plane downstream of the hydraulic jump, defined by $(H_1 - \Delta H)$ remains below the water head plane defined by relationship (53); ΔH denotes the head loss due to the water whirlpool, and $H_1$is the total initial load in section 1. In other words, one may write:

$$H_1 - \Delta H < s + H_c \tag{61}$$

The head loss due to the water whirlpool occurring at the outlet of the convergent decreases as the flow rate increases. For a certain flow rate *Q*, this head loss disappears, and when the liquid stream exits the convergence, it becomes completely free in section 1, i.e., unsubmerged; then, one may write what follows:

$$H_{Up} - H_{Sub} = 0 \tag{62}$$

On the other hand, one can also notice that the liquid vein becomes completely free when inequalities (60) and (61) are transformed into equalities. Under this condition, one may write the following:

$$H_1 - \Delta H = s + H_c \tag{63}$$

Dividing both sides of Eq. (63) by the critical depth h_c, Eq. (17) reduces to:

$$S = \frac{H_1^* - \Delta H^* - H_c / h_c}{h_1^*} \tag{64}$$

Eq. (22) is then reproduced since Eq. (22) and Eq. (64) are the same. However, the latter was derived using a different method based on flow behavior equations.

It is useful to note that for the case of the rectangular channel, the ratio of the total critical head $H_c$to the critical depth h_c is equal to 3/2, i.e.,

$$\frac{H_c}{h_c} = \frac{3}{2} \tag{65}$$

Eq. (64) along with Eq. (65) corresponds to the appearance of the hydraulic jump on the horizontal apron of the channel test; it is satisfied for a flow rate Q_o, and the hydraulic jump originates immediately downstream of the outlet section of the convergent, as depicted in Figs. (5) and (6). Q_o corresponds to the maximum allowable flow rate compatible with the presence of the hydraulic jump. From the moment the flow rate *Q* is increased to become greater than Q_o, the hydraulic jump moves downstream, and the

distance ΔX increases. The initial depth h_1 of the hydraulic jump then corresponds to the final depth of the flow of length ΔX. By again increasing the flow rate Q, the hydraulic jump moves even more downstream. To bring it back to its original position, the sill of height s must be raised. This experimental manipulation aims, in particular, to reduce the length ΔX of the supercritical flow preceding the hydraulic jump as much as possible, whose initial depth h_1 can then be assimilated, with an excellent approximation, to the exit opening a_o. This approach avoids measuring the depth h_1 required for calculating the incident Froude number F_1. The experimental measurement of the initial depth h_1 using a point gauge is very delicate due to the supercritical flow regime.

For a chosen value of the opening a_o and for different sill heights s, the position of the hydraulic jump can also be obtained by a very fine adjustment of the flow rate Q. Laboratory experimentation has shown that this approach is restrictive because a slight increase in the flow rate Q can cause the rapid displacement of the hydraulic jump downstream. For each pair of values (a_o; Q), the incident Froude number F_1 is calculated according to the following relationship:

$$F_1^2 = \frac{Q^2}{g\, b^2\, a_o^3} \tag{66}$$

In fact, each series of tests was carried out for a given opening of the convergent and for different flow rates while maintaining the distance ΔX approximately equal to 5 cm. The length ΔX could not be reduced further due to the horizontal instability of the hydraulic jump. Thus, for fixed a_o and X, different profiles of the hydraulic jump were obtained at increasing flow rates, each corresponding to a given value of the height s of the sill, as shown in Fig. 8.

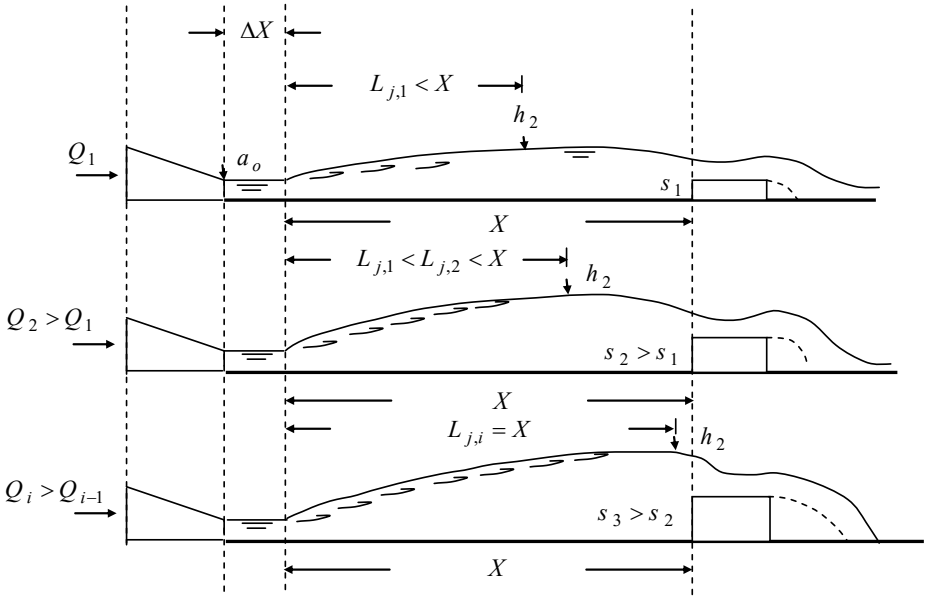

Figure 8: Profiles of the hydraulic jump controlled by a broad-crested sill, obtained at an increasing flow rate Q, while a_o and X are fixed

Description of the test bench and the measurement apparatus

The experiment was carried out in a rectangular channel 40 centimeters wide, 6 meters long and 45 cm deep (Fig. 9) fed in a closed circuit by a 35 l/s flow pump. The walls of the channel are made of transparent glass to visualize the flow, while its bottom is metallic. The double-precision Vernier point gauges intended for the measurement of depths, particularly the final depth h_2, were arranged along the channel by means of metal brackets supported by the walls of the channel (Fig. 11). The double-precision Vernier point gauge used was graduated to 1/10th to minimize reading errors on the depth causing an absolute error of only 0.02 mm. The incident flow is generated by a pressurized convergent 1 m long and of the same width as the test channel. Its initial and final openings are 15 cm and 0.45 cm, respectively, and it is connected to a pressurized box of the same width. The box-converging set, made of sheet metal, is directly supplied by the pump through a flexible pipe. The box and the convergent are fitted inside with carefully arranged guides to best ensure the stability, uniformity, and correct orientation of the incident flow. A waterproof vertical plate is placed above the box and over its entire width to avoid any water overflow when the hydraulic jump is submerged and the measurement channel is flooded (Fig. 9). The flow of water exiting downstream of the test channel was collected in a recovery water basin equipped with a tranquillizer. The basin was connected to the test channel by means of a metal pipe in which the pump is inserted and which ends in a flexible pipe. The diaphragm flow meter is inserted into the steel piping, and its two

pressure taps are connected to a piezometric panel by transparent hoses that allow easy reading of the pressure head. The box-convergent set can move horizontally, which makes it possible to adjust the position X of the sill to the needed value. This operation can also be carried out by moving the sill horizontally, but it is much more restrictive than the first because the sill is carefully fixed and its sealing ensured. The exit opening a_o of the convergent, which has been varied in the range 0.45 cm ≤ a_o ≤ 2.1 cm, was adjusted at will as well as the height s of the sill, which made it possible to obtain a very wide range of values of the relative sill height S such that $1 \leq S \leq 6.15$. The height s of the sill was chosen so that the hydraulic jump forms at a distance ΔX = 5 cm from the convergent generating the incident flow. Sills of different heights, varying between 2.1 cm and 13 cm, were tested associated with previously indicated initial depths $h_1 = a_o$ of the hydraulic jump; these were obtained by operating a simple transverse cut of the convergent at the desired opening a_o by the use of an appropriate metal plate cutting machine.

The adopted openings of the convergent have generated incident Froude numbers varying in the wide range $3.082 \leq F_1 \leq 9.20$.

The flow crossing the sill was free, and the downstream depth h_3 had no influence on the flow rate. The different experimental flow rates were measured by a diaphragm flow meter with a relative error of ± 0.25 l/s. The diaphragm flowmeter has been previously calibrated in the wide range of flow rates Q such that 1.18 l/s ≤ Q ≤ 35 l/s measured using a 90° V-notched weir.

Flow rates Q and depths h_2 were the only parameters requiring specific equipment. The positions X of the sill as well as its height s were simply measured using a graduated tape. As already indicated, the initial depth h_1 of the hydraulic jump was assimilated to the outlet opening a_o of the convergent generating the incident supercritical flow after having positioned the hydraulic jump at approximately ΔX = 5 cm.

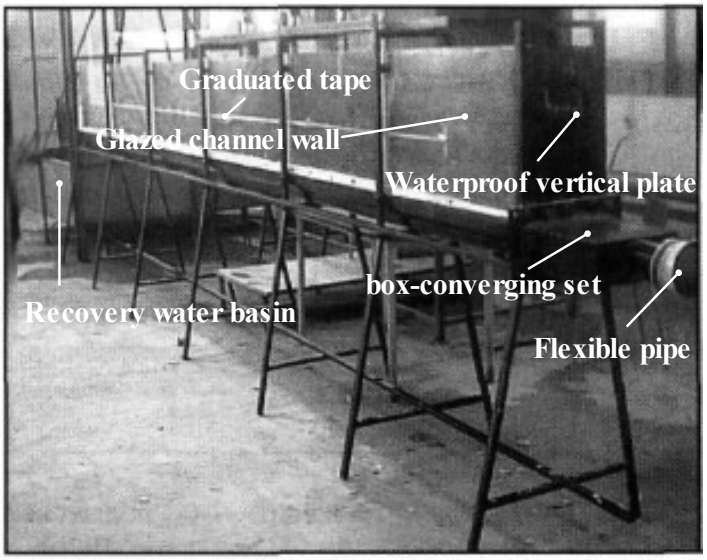

Figure 9: Overview of the rectangular test channel

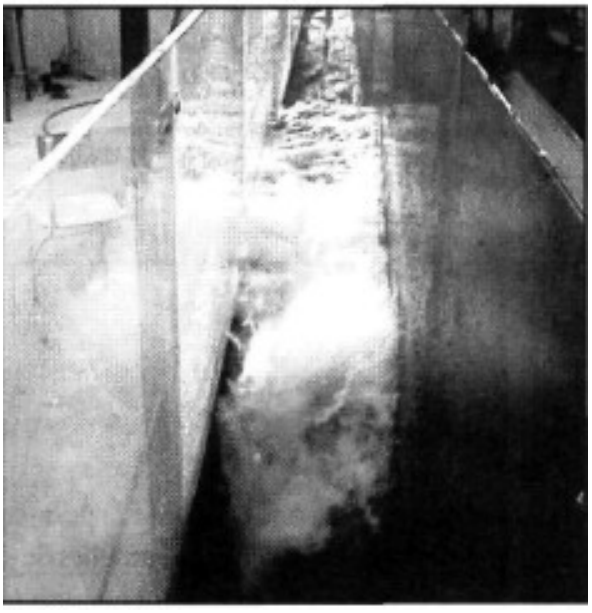

Figure 10: Upstream view of the hydraulic jump

Figure 11: View of the double-precision Vernier point-gauge used for the depth measurement

RESULTS

The experiment was first interested in Eq. (9) of Belanger governing the sequent depth ratio Y of the hydraulic jump as a function of the incident Froude number F_1. The latter was computed using Eq. (66) for each tested opening a_o and flow rate Q. The collected experimental results of Y and F_1 are reported in Table 4, which allows us to plot Fig. 12.

Table 4: Experimental values of Y and F_1 for a hydraulic jump controlled by a broad-crested sill in a rectangular channel

F_1	3.082	3.460	3.950	4.273	4.660	5.423	6.380	6.782	7.322
Y	3.870	4.421	5.120	5.560	6.110	7.150	8.500	9.080	9.800
F_1	7.620	8.240	8.635	9.200					
Y	10.150	11.000	11.650	12.450					

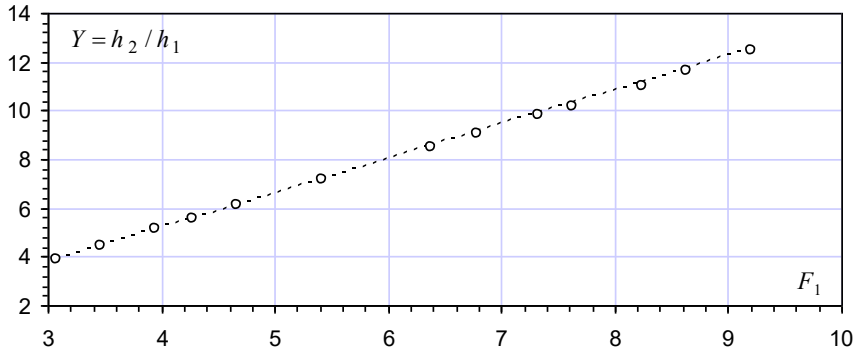

Figure 12: Variation $Y(F_1)$ showing both experimental data (open signs) and theoretical predictions (dashed line) according to Eq. (9).

Fig. 12 clearly shows that the setup of the broad-crested sill on the horizontal apron has practically no reducing effect on the sequent depth ratio Y of the controlled hydraulic jump. Indeed, the experimental points are practically aligned on the Belanger straight dashed line valid for the classical hydraulic jump. For high values of the incident Froude number F_1, it seems that the experimental points tend to lie below the Belanger straight dashed line, meaning that the Y ratio of the controlled jump is lower than the Y ratio of the classical jump. This is probably due to friction effects, but the resulting deviation is not perceptible to the naked eye in Fig. 12. The calculation shows that the maximum deviation between the experimental and theoretical results is less than 1.47% obtained for F_1= 8.24, which allows us to conclude that the theoretical Eq. (9) is generally satisfied in the wide range $3 \leq F_1 \leq 10$. Let us recall that Hager and Bremen (1989) experimentally observed a certain friction effect on the ratio Y for the classic hydraulic jump, which does not appear clearly during our tests.

The variation in the parameters governing the control of the hydraulic jump, such as the relative sill height S and the incident Froude number F_1, was also experimentally examined during our tests. To this must be added the effect of the kinetic factor σ *c*omputed according to Eq. (35) for the known experimental values of Y and F_1. Table 5 groups together the collected experimental values of the involved parameters, particularly showing the theoretical and experimental variation in the kinetic factor σ as a function of the incident Froude number F_1. The variation in σ is clearly observed in Fig. 13.

Table 5: Experimental values of the parameters governing the control of the hydraulic jump by a broad-crested sill in a rectangular channel

F_1	3.082	3.460	3.950	4.273	4.660	5.423	6.380	6.782	7.322
Y	3.870	4.421	5.120	5.560	6.110	7.150	8.500	9.080	9.800
σ	0.317	0.306	0.297	0.295	0.291	0.287	0.281	0.279	0.279
S	1,000	1.290	1.670	1.885	2.200	2.785	3.600	3.950	4.400
F_1	7.620	7.860	7.992	8.170	8.362	8.694	8.841	9.002	9.200
Y	10.150	10.510	10.782	11.000	11.300	11.770	12.000	12.190	12.45
σ	0.282	0.279	0.275	0.276	0.274	0.273	0.271	0.272	0.273
S	4.600	4.850	5.000	5.200	5.400	5.700	5.800	5.950	6.150

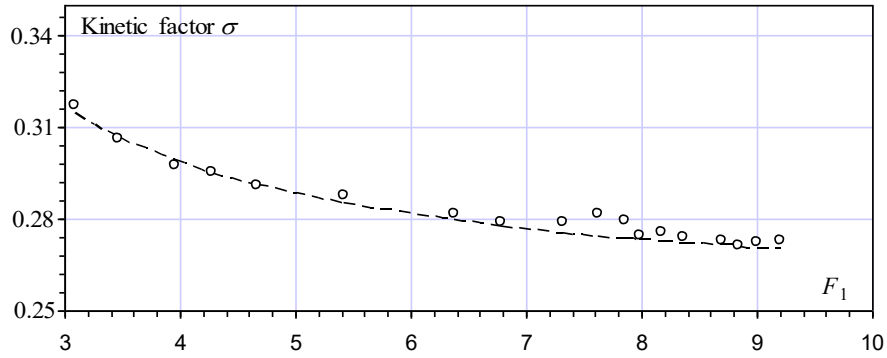

Figure 13: Theoretical and experimental variation in the kinetic factor σ as a function of incident Froude number F_1. (– –) Theoretical Eq. (35); (o) Experimental data

It thus appears that the kinetic factor σ decreases as the incident Froude number increases. For high values of the Froude number F_1, such as $F_1 \geq 6$, the experimental values of σ are slightly higher than the theoretical values and undergo a relatively slow variation around the σ value approximately equal to 0.275. However, it is justified to state that the theoretical relationship (35) that governs the kinetic factor σ is globally satisfied and that the few experimental values that deviate from the theoretical curve were probably affected by some handling errors during the tests. What is interesting to highlight is that the experimental tests confirm that the values of σ are relatively significant so that the kinetic factor cannot be neglected in the theoretical development, as was the case in Forster and Skrinde's study (1950).

On the other hand, Fig. 14 shows both theoretical and experimental variations in the relative sill height S as a function of the incident Froude number F_1.

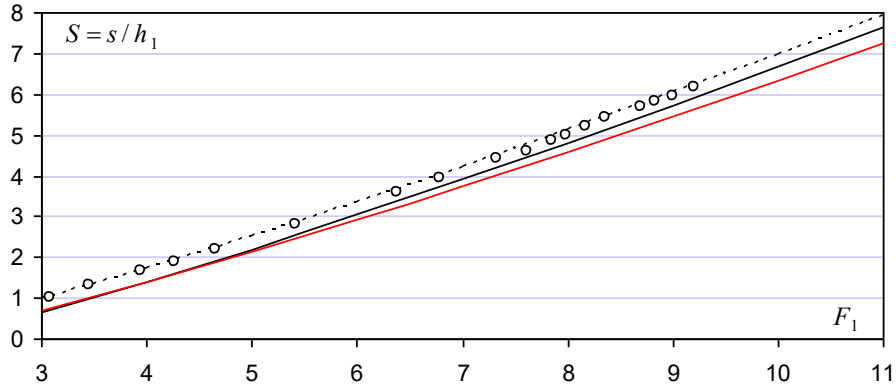

Figure 14: Theoretical and experimental variation in the relative sill height *S* as a function of incident Froude number F_1 during the control of a hydraulic jump by a broad-crested sill in a rectangular channel. (o) Experimental data; (- - -) Authors' theoretical Eq. (33) for $\sigma \neq 0$;

(—) Authors' theoretical Eq. (33) for $\sigma = 0$; (– red curve) Forster and Skrinde's theoretical Eq. (10) neglecting the approach flow velocity (1950).

Fig. 14 shows that the experimental data tend toward the theoretical curve drawn according to the authors' theoretical Eq. (33). One may also observe that the kinetic factor σ is not negligible, especially for low values of the incident Froude number F_1, while its effect is only relative when the values of F_1 are high. Indeed, for high values of F_1, the experimental data come close to the authors' theoretical curve when $\sigma = 0$. However, what it is necessary to point out with regard to Fig. 14 is that the theoretical Forster and Skrinde's Eq. (10) is unreliable, largely because the effect of the approach flow velocity has been wrongly neglected. The second reason is due to the approximation of Eq. (6) on which the theoretical Forster and Skrinde's Eq. (10) is partly based.

As revealed in Fig. 14, Forster and Skrinde's relationship gives values of the relative sill height *S* lower than what they should be. This means that the values of *S* given by Forster and Skrinde's equation will result in releasing the hydraulic jump from the stilling basin to disappear entirely after a moment. Thus, energy dissipation will not occur, and the stilling basin may be damaged due to the erosive effect of the involved forces.

Finally, it is quite justified to conclude that the theoretical relationship (33) derived by the authors can be applied with good accuracy to predict the appropriate relative sill height *S* in the wide range $3 \leq F_1 \leq 9$ and even beyond 9.

CONCLUSION

The study first reviewed the important work of Forster and Skrinde published in 1950 relating to the control of hydraulic jumps by a broad-crested sill in a rectangular channel. Under free-flow conditions, the sill acts as a weir, and the relative sill height S is only a function of the incident Froude number F_1. The dependence between these two variables was translated by an implicit relationship in S whose calculation requires an iterative process [Eq. (10)]. To achieve this relationship, Forster and Skrinde used the momentum equation applied between the final section of the hydraulic jump and the minimum depth section on the sill. However, the theoretical development relies on two simplifying assumptions that have significantly and seriously altered the reliability of the advocated relationship. It is for this reason that the present research has looked at the possibility of finding a more convincing surrogate relationship. Based on the energy equation and on no simplifying assumptions, the authors successfully established the relationship $S(F_1)$ applicable in a wide range of incident Froude numbers such that $3 \leq F_1 \leq 11$ [Eq. (33)]. The double advantage of this relationship lies in the fact that it takes into account the effect of the approach flow velocity and that it is explicit as well, unlike Forster and Skrinde's relationship. This effect is represented by the dimensionless parameter σ defined as a kinetic factor. The calculation showed that for a wide range of incident Froude numbers, the kinetic factor cannot be neglected. A rigorous comparison between the values of the relative sill height S calculated according to Forster and Skrinde and the current approach shows that the maximum deviation observed for $\sigma \neq 0$ is significant, reaching 26.15% for $F_1 = 3$ and 8.41% for $F_1 = 11$. The deviation is 5% when the effect of the approach flow velocity is neglected corresponding to $\sigma = 0$.

This experimental study constituted the second part of the investigations undertaken on the hydraulic jump controlled by a broad-crested sill in a horizontal rectangular channel. The main objective is to corroborate the theoretical relationships or correct them if necessary based on the experimental results. To achieve this objective, broad-crested sills of different heights were tested. After describing the flow and posing the problem, the test bench and measuring equipment were described. This was simple since the experiment only required a diaphragm flowmeter to measure the flow rates and a double-precision Vernier gauge for measuring flow depths, primarily the final depth h_2 of the hydraulic jump. The measurement of the initial depth h_1 of the hydraulic jump was not carried out by a Vernier gauge as it is customary to do. Due to the strongly supercritical nature of the incident flow, the measurement of the depth of this flow by this means is not at all easy and even imprecise. As soon as the tip of the gauge touches the surface of the water, a chaotic jet emerges distorting the reading. This difficulty was circumvented by setting up a pressurized box-convergent set intended to generate the incident flow. The box-convergent combination was directly supplied by a pump via a flexible pipe. The exit opening of the convergent element can be chosen at will according to the needs of the manipulation. The relative position of the sill was chosen so that the hydraulic jump formed immediately downstream of the convergent element, generating the undeveloped incident flow. The exit opening of the convergent was then assimilated, with an excellent

approximation, to the initial depth h_1 of the hydraulic jump. The other advantage of the box-convergent assembly is that it can be moved horizontally on the channel bed, thus making it possible to adjust the position of the sill relative to the exit opening of the convergent according to the handling requirements.

The analysis of the experimental measurements first showed that the sequent depth ratio Y of the hydraulic jump was faithfully defined by Belanger's Eq. (9) even if the hydraulic jump was controlled by a sill. The setup of the broad-crested sill did not affect the ratio Y. Furthermore, experimental measurements have revealed that the relationship (33) is generally reliable over a wide range of incident Froude numbers such that $3 \leq F_1 \leq 9$. A comparative study showed that the relationship (10) of Forster and Skrinde was not recommendable. It gives lower sill heights than they should be and thus will probably cause the disappearance of the hydraulic jump from the stilling basin, whose security would be seriously threatened by the erosive effects of the opposing forces. These same experimental measurements showed above all that the kinetic factor σ could not be neglected, as it was unfairly considered in the previous works of Forster and Skrinde. It was observed that the kinetic factor σ decreased as the incident Froude number F_1 increased. For high values of F_1, such as $F_1 \geq 6$, the experimental σ was slightly higher than the theoretical σ and underwent a slight variation around the mean value $\sigma = 0.275$.

Declaration of competing interest

The authors declare that they have no known competing financial interests or personal relationships that could have appeared to influence the work reported in this paper.

REFERENCES

ACHOUR B. (1997). Hydraulic jump energy dissipators, State Doctorate Thesis in Sciences, University of Tizi-Ouzou, Algeria. (In French)

ACHOUR B., (2000). Hydraulic jump in a suddenly widened circular tunnel, Journal of Hydraulic Research, Vol. 38, Issue 4, pp. 307-311.

ACHOUR B., DEBABÈCHE M. (2003a). Control of hydraulic jump by sill in triangular channel, Journal of Hydraulic Research, Vol. 41, Issue 3, pp. 319-325. (In French)

ACHOUR B., DEBABÈCHE M. (2003b). Control of hydraulic jump by sill in a U-shaped channel, Journal of Hydraulic Research, Vol. 41, Issue 1, pp. 97-103. (In French)

ACHOUR B., SEDIRA N., DEBABECHE M. (2002). Control of hydraulic jump by sill in a rectangular channel, Larhyss Journal, No 1, pp. 1-14. (In French)

BELANGER J.B. (1828). Essay on the numerical solution of some problems relating to the permanent movement of running water, Carilian-Goeury, Paris, France. (In French)

BRETZ N.V. (1988). Forced hydraulic jump by sill, Laboratory of Hydraulic Constructions, Federal Polytechnic School of Lausanne, Department of Civil Engineering, Communication No. 2. (In French).

DOERINGSFELD H.A., C.L. BARKER C.L. (1941). Pressure-Momentum Theory Applied to the Broad-Crested Weir, Transactions American Society of Civil Engineering, ASCE, Vol. 106, Issue 1, pp. 934-969.

FORSTER J.W., SKRINDE R.A. (1950). Control of the hydraulic jump by sills, Transactions American Society of Civil Engineering, ASCE, Vol. 115, pp. 973-987.

HAGER W.H., BREMEN R., KAWAGOSHI N. (1990). Classical Hydraulic Jump – Length of Roller, Journal of Hydraulic Research, Vol. 28, Issue 5, pp. 591-608.

HAGER W.H., LI D. (1992). Sill-controlled energy dissipator, Journal of Hydraulic Research, Vol. 30, Issue 2, pp. 165-181.

HAGER W.H., WANOSCHEK R. (1987). Hydraulic jump in triangular channel, Journal of Hydraulic Research, Vol. 25, Issue 5, pp. 549-564.

KAWAGOSHI N., HAGER W.H. (1989). B-jump in sloping channel, II, Journal of Hydraulic Research, Vol. 28, Issue 4, pp. 461-480.

KOLB W.M. (1983). Curve fitting for programmable calculators, 2nd Edition, Published by IMTEC, Bowi, Maryland, USA.

McCORQUODALE J.A., MOHAMED M.S. (1994). Hydraulic jump on adverse slope, Journal of Hydraulic Research, Vol. 32, Issue 4, pp. 119-130.

NANDAVA V., AYED M.A.G. (1992). Modified type III stilling basin – New method of design, Journal of Hydraulic Research Vol. 30, Issue 4, pp. 485-498.

PETERKA A.J. (1983). Hydraulic design of stilling basins and energy dissipators, Water Resources Technical Publications, Engineering Monograph No. 25, USBR, United States Bureau of reclamation, Denver, Colorado, USA.

RAO N.S.G., MURALIDHAR D. (1963). Discharge characteristics of weirs of limit crest width, La Houille Blanche, No 18, pp. 537-545.

SMITH C.D., CHEN W. (1989). The hydraulic jump in a steeply sloping square conduit, Journal Hydraulic Research, Vol. 27, Issue 3, pp. 301-319.